J. Fluid Mech. (1990), *vol.* 221, *pp.* 263–288
Printed in Great Britain

The extended Korteweg–de Vries equation and the resonant flow of a fluid over topography

By T. R. MARCHANT AND N. F. SMYTH
Department of Mathematics, The University of Wollongong, PO Box 1144, Wollongong, NSW 2500, Australia

(Received 2 August 1989 and in revised form 20 March 1990)

The extended Korteweg–de Vries equation which includes nonlinear and dispersive terms cubic in the wave amplitude is derived from the water-wave equations and the Lagrangian for the water-wave equations. For the special case in which only the higher-order nonlinear term is retained, the extended Korteweg–de Vries equation is transformed into the Korteweg–de Vries equation. Modulation equations for this equation are then derived from the modulation equations for the Korteweg–de Vries equation and the undular bore solution of the extended Korteweg–de Vries equation is found as a simple wave solution of these modulation equations. The modulation equations are also used to extend the solution for the resonant flow of a fluid over topography. This resonant flow occurs when, in the weakly nonlinear, long-wave limit, the basic flow speed is close to a linear long-wave phase speed for one of the long-wave modes. In addition to the effect of higher-order terms, the effect of boundary-layer viscosity is also considered. These solutions (with and without viscosity) are compared with recent experimental and numerical results.

1. Introduction

Many equations describing nonlinear wave motions have exact solutions for steady uniform progressive waves. However, such steady waves do not usually exist and methods are needed to study modulated wavetrains. One such method which has had wide application in the study of slowly varying wavetrains is the averaged Lagrangian method of Whitham (1965*a*, *b*, 1967, 1974). This method involves deriving modulation equations for slowly varying wave properties such as amplitude, mean height, frequency and wavenumber from a Lagrangian for the wave system averaged over a period. This method has been successfully applied to a wide variety of nonlinear wave systems, in particular the Korteweg–de Vries equation (Whitham, 1965*b*, 1974). The modulation equations for the Korteweg–de Vries equation are found to form a third-order system of hyperbolic equations for the amplitude, wavenumber, frequency and mean height. Since the modulation equations are hyperbolic, the cnoidal wave solution of the Korteweg–de Vries equation is stable to small modulations. A particular solution of these equations, a simple wave solution, was found by Gurevich & Pitaevskii (1974), this solution corresponding physically to an undular bore. This undular bore solution was found to be in good agreement with numerical solutions of the Korteweg–de Vries equation by Fornberg & Whitham (1978). It is an extension of this work to an extended Korteweg–de Vries equation which forms the first portion of the present work.

The Korteweg–de Vries equation arises in the description of weakly nonlinear, long wavelength water waves when terms of second order in wave amplitude in the water-

wave equations are included (see Whitham 1974). In §2, the extended Korteweg–de Vries equation, which includes terms of third order in wave amplitude, is derived in two ways; the first is an extension of the derivation of Whitham (1974) of the Korteweg–de Vries equation from the water-wave equations and the second is from the Lagrangian for the water-wave equations derived by Luke (1967). Since a Lagrangian for the extended Korteweg–de Vries equation is required to apply modulation theory, the second method of derivation is useful as it leads directly to this Lagrangian. Deriving the modulation equations for the full extended Korteweg–de Vries equation,

$$\eta_t+6\eta\eta_x+\eta_{xxx}-\alpha c_1\eta^2\eta_x+\alpha c_2\eta\eta_{xxx}+\alpha c_3\eta_x\eta_{xx}+\alpha c_4\eta_{xxxxx}=0, \tag{1.1}$$

where c_1, c_2, c_3 and c_4 are constants and $\alpha \ll 1$ is the amplitude-to-depth ratio, presents significant algebraic difficulty. In §2 it is shown that the extended Korteweg–de Vries equation containing only the higher-order nonlinear term and not the higher-order dispersive terms,

$$\eta_t+6\eta\eta_x+\eta_{xxx}-\alpha c_1\eta^2\eta_x=0, \tag{1.2}$$

can be transformed to the Korteweg–de Vries equation for $\alpha \ll 1$. The modulation equations for (1.2) then follow from the modulation equations for the Korteweg–de Vries equation. These modulation equations thus form a third-order system of hyperbolic equations for the mean height, wavenumber and amplitude, as do the modulation equations for the Korteweg–de Vries equation. A higher-order undular bore solution is found as a simple wave solution of these modulation equations and is compared with the numerical undular bore solution of (1.2).

The modulation equations for (1.2) are used in §3 to derive the higher-order solution for the resonant flow of a fluid over topography. The method of solution parallels that of Smyth (1987) for the Korteweg–de Vries equation. This flow occurs when the basic flow speed is near one of the linear long-wave speeds for one of the long-wave modes, so that energy cannot escape from the topographic forcing at the linear group velocity and nonlinear effects become important (indeed dominant) in the resulting flow. This resonant flow was first derived experimentally by Huang *et al.* (1982) and since then has been considered both theoretically (Wu & Wu 1982; Akylas 1984; Cole 1985; Lee 1985; Grimshaw & Smyth 1986; Melville & Helfrich 1987; Smyth 1987, 1988; Wu 1987; Lee, Yates & Wu 1989) and experimentally (Baines 1984; Lee 1985; Melville & Helfrich 1987; Lee *et al.* 1989). Both experimentally and theoretically, it is found that the resonant flow consists of three distinct regions (see figure 2). Upstream of the forcing, there is an advancing train of waves, these waves being generated at the forcing. Downstream of the forcing, there is a lengthening depression of nearly constant depth followed by a modulated wavetrain which brings the flow back to zero. Akylas (1984), Cole (1985), Lee (1985) and Grimshaw & Smyth (1986) showed that to second order in wave amplitude, this flow can be described by the forced Korteweg–de Vries equation. Melville & Helfrich (1987) showed that when third-order nonlinear terms are included, the flow is governed by the forced extended Korteweg–de Vries equation.

Most of the theoretical work done to date has involved numerical solutions. Grimshaw & Smyth (1986) approximated the upstream wavetrain by a series of constant amplitude Korteweg–de Vries solitons and using mass and energy balance arguments, found expressions for the soliton amplitude and spacing which agreed well with numerical solutions near exact linear resonance. For the downstream

wavetrain, the undular bore solution of the Korteweg–de Vries equation was used and good agreement was found with numerical solutions over the entire resonant range. Smyth (1987) improved the upstream solution by showing that it is a partial undular bore. The upstream wavetrain is then a modulated cnoidal wave at whose leading edge, the modulus squared $m = 1$, so that it is essentially a train of solitons there, and at whose trailing edge at the forcing, $m = m_0$, where $1 > m_0 \geqslant 0$. In a full undular bore, $m = 0$ at the trailing edge of the bore. Waves of modulus squared m_0 are chosen so that the expansion fan for the simple wave (undular bore) solution of the modulation equations for the Korteweg–de Vries equation has zero velocity at the forcing and hence the entire wavetrain propagates upstream. This upstream solution was found to be in good agreement with numerical solutions for the entire resonant range. In §3, the resonant flow solution of the forced extended Korteweg–de Vries equation will be found using the method of Smyth (1987) and the results compared with the experimental results of Melville & Helfrich (1987).

The difference between the experimental and theoretical amplitudes of the waves in the resonant flow is about 10%. One of the motivations for considering higher-order corrections to the Korteweg–de Vries equation is to determine the effect of these higher-order terms relative to the effect of viscosity in explaining this difference. Smyth (1988) considered the effect of viscosity and found that it accounts for a portion of the difference between the experimental and theoretical results. By solving the full forced extended Korteweg–de Vries equation numerically, it is found in §4 that the effects of viscosity are more important than the effects of higher-order nonlinearity and dispersion in accounting for the differences between experimental and theoretical results.

2. Extended Korteweg–de Vries equation

2.1. *Derivation of the equation*

The Korteweg–de Vries equation is obtained as an extension to the linear shallow-water equations when the effects of the next higher-order nonlinearity and dispersion are included, these terms being $O(\alpha^2)$ where α is a measure of the amplitude. The extended Korteweg–de Vries equation, obtained by including nonlinear, dispersive and mixed nonlinear–dispersive terms to $O(\alpha^3)$, will be derived in two ways in the present section; the first is an extension of the derivation of Whitham (1974) from the water-wave equations and the second is from the Lagrangian for the water-wave equations found by Luke (1967). The second derivation is useful as to apply the averaged Lagrangian method of Whitham (1974) to the extended Korteweg–de Vries equation, a Lagrangian for this equation is needed.

Let us consider small-amplitude, long-wavelength, two-dimensional waves propagating on the surface of an incompressible, inviscid, irrotational fluid of undisturbed constant depth h. All space variables will be non-dimensionalized by h and the time will be non-dimensionalized by $(hg^{-1})^{\frac{1}{2}}$, where g is the acceleration due to gravity. The horizontal coordinate will be denoted by X, the vertical coordinate by Y, the time by T, the velocity potential by Φ and the surface elevation by N. Since the waves are assumed to be of small amplitude and long wavelength, we set

$$\left.\begin{aligned} X &= \beta^{-\frac{1}{2}}x, \quad T = \beta^{-\frac{1}{2}}t, \\ N &= \alpha\eta, \quad \Phi = \alpha\beta^{-\frac{1}{2}}\phi, \end{aligned}\right\} \tag{2.1}$$

where

$$\left.\begin{aligned}\alpha &= \frac{a}{h},\\ \beta &= \left(\frac{h}{l}\right)^2,\end{aligned}\right\} \tag{2.2}$$

a being a typical wave amplitude and l a typical wavelength. The water-wave equations then become (see Whitham 1974)

$$\left.\begin{aligned}\beta\phi_{xx}+\phi_{YY} &= 0 \quad (0<Y<1+\alpha\eta),\\ \phi_Y &= 0 \quad \text{on} \quad Y=0,\end{aligned}\right\}$$
$$\left.\begin{aligned}\eta_t+\alpha\phi_x\eta_x-\beta^{-1}\phi_Y &= 0\\ \eta+\phi_t+\tfrac{1}{2}\alpha\phi_x^2+\tfrac{1}{2}\alpha\beta^{-1}\phi_Y^2 &= 0\end{aligned}\right\} \quad \text{on} \quad Y=1+\alpha\eta. \tag{2.3}$$

The velocity potential ϕ is expanded as a series in β as

$$\phi = \sum_{m=0}^{\infty}(-1)^m\beta^m\frac{Y^{2m}}{(2m)!}\frac{\partial^{2m}f}{\partial x^{2m}}, \tag{2.4}$$

which satisfies Laplace's equation and the boundary condition at $Y=0$. Substituting (2.4) into the surface boundary conditions of (2.3) yields on retaining terms up to and including $O(\alpha^2,\alpha\beta,\beta^2)$.

$$\left.\begin{aligned}\eta_x+f_{xt}+\alpha\eta\eta_x+\tfrac{1}{2}\beta\eta_{xxx}-\tfrac{3}{4}\alpha^2\eta^2\eta_x+\alpha\beta(\tfrac{10}{3}\eta_x\eta_{xx}+\tfrac{4}{3}\eta\eta_{xxx})+\tfrac{5}{24}\beta^2\eta_{xxxxx} &= 0,\\ \eta_t+f_{xx}+2\alpha\eta\eta_x-\tfrac{1}{6}\beta\eta_{xxx}-\tfrac{3}{4}\alpha^2\eta^2\eta_x+\alpha\beta(\tfrac{1}{12}\eta_x\eta_{xx}-\tfrac{1}{12}\eta\eta_{xxx})-\tfrac{2}{45}\beta^2\eta_{xxxxx} &= 0.\end{aligned}\right\} \tag{2.5}$$

The function f_x is now chosen so that both of (2.5) are the same equation. Retaining terms to $O(\alpha,\beta)$, Whitham (1974) found

$$f_x = \eta-\tfrac{1}{4}\alpha\eta^2+\tfrac{1}{3}\beta\eta_{xxx}, \tag{2.6}$$

which gives the Korteweg–de Vries equation. For the extended equation (2.5), which includes terms of next highest order, we find

$$f_x = \eta-\tfrac{1}{4}\alpha\eta^2+\tfrac{1}{3}\beta\eta_{xxx}+\tfrac{1}{8}\alpha^2\eta^3+\alpha\beta(\tfrac{3}{16}\eta_x^2+\tfrac{1}{2}\eta\eta_{xx})+\tfrac{1}{10}\beta^2\eta_{xxxx}, \tag{2.7}$$

which gives the extended Korteweg–de Vries equation

$$\eta_t+\eta_x+\tfrac{3}{2}\alpha\eta\eta_x+\tfrac{1}{6}\beta\eta_{xxx}-\tfrac{3}{8}\alpha^2\eta^2\eta_x+\alpha\beta(\tfrac{23}{24}\eta_x\eta_{xx}+\tfrac{5}{12}\eta\eta_{xxx})+\tfrac{19}{360}\beta^2\eta_{xxxxx} = 0. \tag{2.8}$$

This extended equation contains a higher-order nonlinear term of $O(\alpha^2)$, higher-order mixed nonlinear–dispersive terms of $O(\alpha\beta)$ and a higher-order dispersive term of $O(\beta^2)$. As usual, to balance the nonlinear and dispersive terms, we assume $\alpha=\beta$. An extended Korteweg–de Vries equation can also be obtained for the more general case of weakly nonlinear long waves in a stratified fluid and an equation similar to (2.8) will be obtained, with different coefficients (see Gear & Grimshaw 1983).

The extended Korteweg–de Vries equation (2.8) can also be obtained directly from the Lagrangian for the water-wave equations, this Lagrangian being found by Luke (1967). Using the scalings (2.1), this Lagrangian becomes

$$\frac{L}{\rho hga} = \int_0^{1+\alpha\eta}[\phi_t+\tfrac{1}{2}\alpha\phi_x^2+\tfrac{1}{2}\alpha\beta^{-1}\phi_Y^2]\,\mathrm{d}Y+\tfrac{1}{2}\alpha\eta^2. \tag{2.9}$$

On substituting the expansion (2.4) for ϕ into this Lagrangian and retaining terms of $O(\alpha^3, \alpha\beta^2, \alpha^2\beta)$, we find

$$\frac{L}{\rho g h a} = f_t + \alpha\eta f_t + \tfrac{1}{2}\alpha\eta^2 - \tfrac{1}{6}\beta f_{xxt} + \tfrac{1}{2}\alpha f_x^2 - \tfrac{1}{2}\alpha\beta\eta f_{xxt} + \tfrac{1}{6}\alpha\beta f_{xx}^2 + \tfrac{1}{120}\beta^2 f_{xxxxt}$$
$$+ \tfrac{1}{2}\alpha^2\eta f_x^2 - \tfrac{1}{6}\alpha\beta f_x f_{xxx} - \tfrac{1}{2}\alpha^2\beta\eta^2 f_{xxt} + \tfrac{1}{24}\alpha\beta^2\eta f_{xxxxt} + \tfrac{1}{2}\alpha^2\beta\eta f_{xx}^2 - \tfrac{1}{30}\alpha\beta^2 f_{xx} f_{xxxx}$$
$$- \tfrac{1}{2}\alpha^2\beta\eta f_{xxx} f_x + \tfrac{1}{120}\alpha\beta^2 f_x f_{xxxxx} + \tfrac{1}{40}\alpha\beta^2 f_{xxx}^2. \quad (2.10)$$

We have
$$L = L(y, f, f_t, f_x, f_{xx}, f_{xxt}, f_{xxx}, f_{xxxx}, f_{xxxxt}, f_{xxxxx}), \quad (2.11a)$$

and hence (see Whitham 1974, §11) the variational equations for this Lagrangian are

$$\left.\begin{aligned} L_\eta &= 0, \\ L_f \frac{\partial}{\partial t}(L_{ft}) - \frac{\partial}{\partial x}(L_{fx}) + \frac{\partial^2}{\partial x^2}(L_{fxx}) - \frac{\partial^3}{\partial x^2 \partial t}(L_{fxxt}) & \\ - \frac{\partial^3}{\partial x^3}(L_{fxxx}) + \frac{\partial^4}{\partial x^4}(L_{fxxxx}) - \frac{\partial^5}{\partial x^4 \partial t}(L_{fxxxxt}) - \frac{\partial^5}{\partial x^5}(L_{fxxxxx}) &= 0. \end{aligned}\right\} \quad (2.11b)$$

By differentiating the first of (2.11*b*) and after some algebra, we obtain (2.5) and hence the full extended Korteweg–de Vries equation follows as before.

2.2. *Modulation equations and the simple wave solution*

The extended Korteweg–de Vries equation (2.8) has been derived for the special case of surface waves. If we had derived an extended Korteweg–de Vries equation for the more general case of waves in a density stratified fluid, then the equation would have had the same form as (2.8), but with different coefficients, i.e.

$$\eta_t + \mu_1 \alpha\eta\eta_x + \mu_2 \beta\eta_{xxx} - \alpha^2\bar{c}_1 \eta^2\eta_x + \alpha\beta\bar{c}_2 \eta_x \eta_{xx} + \alpha\beta\bar{c}_3 \eta\eta_{xxx} + \beta^2\bar{c}_4 \eta_{xxxxx} = 0, \quad (2.12)$$

where μ_1, μ_2, $\bar{c}_1$, $\bar{c}_2$, $\bar{c}_3$ and $\bar{c}_4$ are constants which depend on the density stratification (see (2.8) for surface waves). An equation of the form (2.12) was derived by Chow (1989) for the case of surface waves on a fluid with an underlying shear flow. The coefficients μ_1, μ_2, $\bar{c}_1$, $\bar{c}_2$, $\bar{c}_3$ and $\bar{c}_4$ were given as the solutions of a set of boundary-value problems for ordinary differential equations, and were explicitly evaluated for the case of a linear shear flow.

Some special cases occur, however, which change the form of (2.12). In particular, if μ_1 becomes small, i.e. $\mu_1 = O(\alpha^n)$ where $0 < n \leqslant 1$, then in order to match the leading-order nonlinearity and dispersion, we require $\beta = O(\alpha^{n+1})$. Hence in this special case higher-order nonlinearity becomes more important than higher-order dispersion. Now, for surface waves the matching of leading-order nonlinearity and dispersion requires the usual scaling $\beta = O(\alpha)$. For the special case $\mu_1 = O(\alpha^n)$, however, we retain only the cubic nonlinearity (which remains $O(\alpha^2)$), while the mixed nonlinear–dispersive terms, $O(\alpha^{n+1})$, and higher-order dispersion, $O(\alpha^{2+2n})$, are ignored as they are of higher order in α. This gives (after scaling) an extended Korteweg–de Vries equation containing only the higher-order nonlinear term

$$\eta_t + 6\eta\eta_x + \eta_{xxx} - \alpha c_1 \eta^2\eta_x = 0, \quad (2.13)$$

where $\alpha c_1 \ll 1$ for $0 < n < 1$ and $\alpha c_1 = O(1)$ for $n = 1$.

While equation (2.13) is more limited in its applicability than (2.12), it is a valid approximation in a number of physical situations. Melville & Helfrich (1987)

implicitly assume $\beta = O(\alpha^{n+1})$ for $n > 0$ and derive a form of equation (2.13) for two-layer flow. They add topographic forcing to analyse the resonant or transcritical flow of a two-layer fluid over topography. This flow occurs when the basic flow speed is near a linear long-wave speed for one of the long-wave modes, so that energy cannot escape from the topographic forcing at the linear group velocity and nonlinear effects become important (indeed dominant) in the resulting flow. This flow will be further discussed in §3. Other examples of flows where (2.13) occurs are a fluid with uniform stratification in the absence of a basic shear flow in the Boussinesq approximation (Gear & Grimshaw 1983) and a two-layer fluid when the two depths are nearly the same (Long 1956; Kakutani & Yamasaki 1978; Helfrich, Melville & Miles 1984; Miles 1979). For two-layer fluids, when the depths of the two layers are nearly the same, the scaling assumption is $\beta = O(\alpha^2)$, which causes the two nonlinear terms in (2.13) to be of the same order, i.e. $\alpha c_1 = O(1)$.

Finding the modulation equations for (2.12) presents significant algebraic difficulties. However, on using a transformation presented below, the modulation equations for the extended Korteweg–de Vries equation containing only the higher-order nonlinear term (2.13) can be easily found. This transformation involves transforming (2.13) to the Korteweg–de Vries equation for $\alpha c_1 \ll 1$, from which the modulation equations follow from those of the Korteweg–de Vries equation found by Whitham (1965*b*, 1974). It should be noted however that this transformation is not strictly valid for $\alpha c_1 = O(1)$, which reduces the value of comparisons of this theory with the results from cases where $\beta = O(\alpha^2)$.

If we let

$$\eta = \eta_v + \frac{\alpha c_1}{12}(2\eta_v^2 + \eta_{vxx}), \tag{2.14}$$

then η_v is the solution of the Korteweg–de Vries equation (terms of $O(\alpha^2)$ being neglected),

$$\eta_{vt} + 6\eta_v \eta_{vx} + \eta_{vxxx} = 0. \tag{2.15}$$

This transformation only eliminates higher-order terms of the form $\eta^2\eta_x$ and $\eta_x\eta_{xx}$, so the full extended Korteweg–de Vries equation (2.12) cannot be transformed to the Korteweg–de Vries equation by this method. The modulation equations for the Korteweg–de Vries equation (2.15) are given by Whitham (1965*b*, 1974) as

$$\left.\begin{aligned}
P\colon\quad & 2\beta_v + \frac{4a_v(K(m)-E(m))}{mK(m)} - 2a_v - \frac{2a_v}{m} = \text{constant} \\
& \text{on} \quad \frac{\mathrm{d}x}{\mathrm{d}t} = U - \frac{4a_v K(m)}{K(m)-E(m)}, \\
Q\colon\quad & 2\beta_v + \frac{4a_v(K(m)-E(m))}{mK(m)} - \frac{2a_v}{m} = \text{constant} \\
& \text{on} \quad \frac{\mathrm{d}x}{\mathrm{d}t} = U - \frac{4a_v(1-m)K(m)}{E(m)-(1-m)K(m)}, \\
R\colon\quad & 2\beta_v + \frac{4a_v(K(m)-E(m))}{mK(m)} - 2a_v = \text{constant} \\
& \text{on} \quad \frac{\mathrm{d}x}{\mathrm{d}t} = U + \frac{4a_v(1-m)K(m)}{mE(m)},
\end{aligned}\right\} \tag{2.16}$$

where the phase speed U of cnoidal waves is

$$U = 6\beta_v + 4a_v\left(\frac{2}{m} - 1 - \frac{3E(m)}{mK(m)}\right), \tag{2.17}$$

and the wavenumber k is

$$k = \frac{\pi a_v^{\frac{1}{2}}}{m^{\frac{1}{2}}K(m)}. \tag{2.18}$$

These equations form a third-order hyperbolic system of equations for the amplitude a_v, mean height β_v and modulus squared m of the modulated cnoidal wave

$$\eta_v = \beta_v + 2a_v\left[\frac{1-m}{m} - \frac{E(m)}{mK(m)} + \mathrm{cn}^2\left(\frac{K(m)\,\theta}{\pi}\right)\right], \tag{2.19}$$

θ being the phase. $K(m)$ and $E(m)$ are complete elliptic integrals of the first and second kind of modulus squared m respectively.

The relationship between the wave amplitude a_v and mean height β_v and the wave amplitude a and mean height β of the extended Korteweg–de Vries equation (2.13) can be found from (2.19) and the transformation (2.14) to be

$$\left.\begin{aligned} a &= a_v + \frac{\alpha c_1}{6}\left[2\beta_v a_v - a_v^2 + \frac{2a_v^2}{m} - \frac{4a_v^2}{m}\frac{E(m)}{K(m)}\right], \\ \beta &= \beta_v + \frac{\alpha c_1}{6}\left[\beta_v^2 + \frac{4a_v^2}{m^2}\left(\frac{E(m)}{K(m)} - 1 + m\right)\left(m - \frac{E(m)}{K(m)}\right)\right. \\ &\quad \left. - \frac{4}{3}\frac{a_v^2}{m^2}\left(1 - 4m + 3m^2 + (2m-1)\frac{E(m)}{K(m)}\right)\right]. \end{aligned}\right\} \tag{2.20}$$

The phase speed U and wavenumber k of the modulated cnoidal wave solution of the extended Korteweg–de Vries equation (2.13) are given by (2.17) and (2.18) when β_v and a_v are replaced by β and a using (2.20). The periodic travelling-wave solution of the extended Korteweg–de Vries equation (2.13) follows upon substitution of the cnoidal wave solution (2.19) for the Korteweg–de Vries equation into the transformation (2.14).

An alternative approach to deriving the modulation equations for the full extended Korteweg–de Vries equation (2.12) is to perturb the inverse scattering solution of the Korteweg–de Vries equation. Byatt-Smith (1987), using the results of Kaup & Newell (1978), constructed solutions of perturbed Korteweg–de Vries equations from the inverse scattering solution of the Korteweg–de Vries equation. This method could be applied to the modulation equations for the Korteweg–de Vries equation as derived using inverse scattering by Flaschka, Forest & McLaughlin (1980).

One particular solution of the modulation equations (2.16) that can be easily found is the simple wave solution on the characteristic Q. This solution was first found by Gurevich & Pitaevskii (1974) and Fornberg & Whitham (1978) and corresponds physically to an undular bore. This solution, which is unsteady, is referred to as an undular bore since it corresponds to a smoothing out of an initial step function. There are also models of undular bores which are steady owing to the effect of friction (see Whitham 1974, §13.15) which are not to be confused with the undular bores referred to in the present work. Using the relations (2.20), this undular bore solution can be easily extended to the extended Korteweg–de Vries equation (2.13). Using

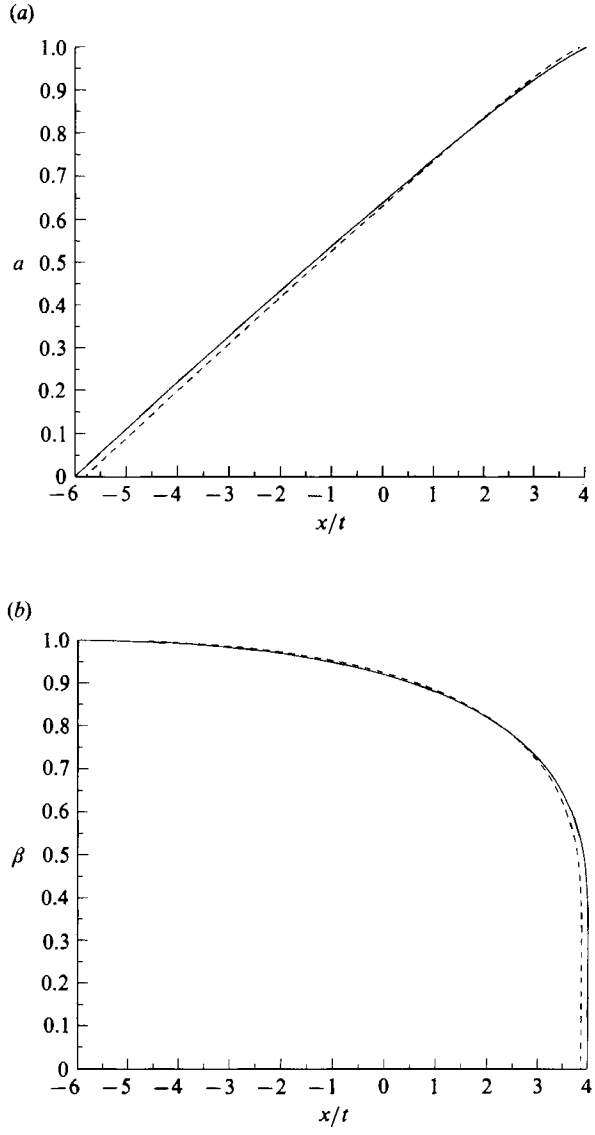

FIGURE 1 (*a*, *b*). For caption see facing page.

(2.16)–(2.18) and (2.20), the undular bore solution of (2.13) linking the level A behind the bore to the level B ahead of the bore is then

$$a = (A-B)\,m - \tfrac{1}{6}\alpha c_1 (A-B)^2 m(1-m),$$

$$\beta = 2B - A + 2(A-B)\frac{E(m)}{K(m)} + (A-B)\,m + \tfrac{1}{18}\alpha c_1 (A-B)^2 \left[3m^2 - 5m + 2 + 2(2m-1)\frac{E(m)}{K(m)}\right],$$

$$k = \frac{\pi}{K(m)}(A-B)^{\frac{1}{2}}[1 - \tfrac{1}{12}\alpha c_1 (A+B)],$$

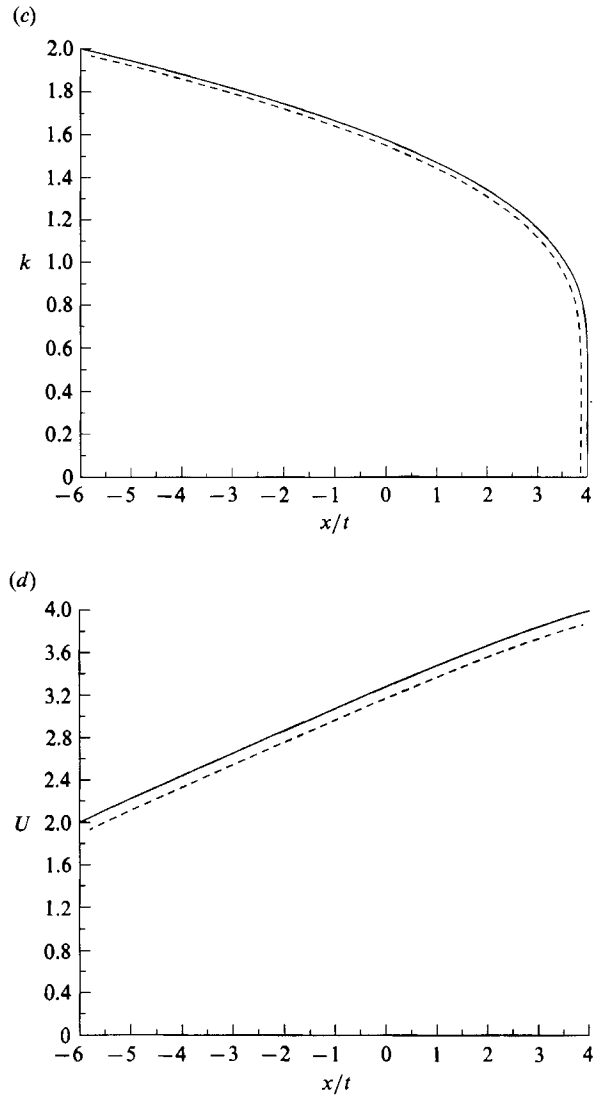

FIGURE 1. (*a*) The amplitude a of the undular bore versus x/t for a jump from $B = 0$ to $A = 1$. Compared are ---, the extended Korteweg–de Vries equation for $\alpha c_1 = 0.2$ and the ——, the Korteweg–de Vries equation. Also shown for the same situation as (*a*) are (*b*) mean height β, (*c*) wavenumber k, and (*d*) phase speed U.

$$U = 6B + 2(A-B)(1+m) - \tfrac{1}{3}\alpha c_1[3(2B-A)^2 + 2(A-B)(2B-A)(4+m) + 3(A-B)^2(2+m)],$$

on $$\frac{x}{t} = U - \frac{2(A-B)\,m(1-m)\,K(m)}{E(m)-(1-m)\,K(m)}[2-\tfrac{1}{3}\alpha c_1(A+B)], \quad 0 \leqslant m \leqslant 1,$$

$$12B - 6A + \alpha c_1(A^2-2B^2) \leqslant \frac{x}{t} \leqslant 2B + 4A - \tfrac{1}{3}\alpha c_1(B^2+2A^2). \quad (2.21)$$

The undular bore is a modulated cnoidal wavetrain which has solitons ($m = 1$) of amplitude $2(A-B)$ on a mean height B at the leading edge of the fan and sinusoidal

waves of small amplitude on mean height A at the trailing edge of the fan. From (2.21) it can be seen that the leading edge of the extended undular bore moves slower (for $c_1 > 0$) than the leading edge of the undular bore solution for the Korteweg–de Vries equation. The trailing edge of the extended undular bore moves faster than the trailing edge of the Korteweg–de Vries undular bore if $|A| < \sqrt{2}|B|$ and slower if $|A| > \sqrt{2}|B|$.

Figure 1(*a*) shows a comparison of the amplitude of the extended undular bore solution and the Korteweg–de Vries undular bore solution versus x/t for a jump from $B = 0$ to $A = 1$. First, for this case the trailing edge of the extended undular bore has a smaller speed than the Korteweg–de Vries undular bore and the leading edge also has a smaller speed. Hence the extended undular bore spreads out more slowly than the Korteweg–de Vries undular bore. The amplitude of both bores goes from zero at the trailing edge to 1 at the leading edge. Hence because of the different positions of the trailing and leading edges, the amplitude of the extended undular bore is slightly lower near the trailing edge and slightly higher near the leading edge. Figure 1(*b*) shows a comparison of the mean heights for the same parameters as in figure 1(*a*). Both of the mean heights go from 1 at the trailing edge to zero at the leading edge. So the mean height of the extended undular bore is slightly higher near the trailing edge and slightly lower near the leading edge of the undular bore. Figures 1(*c*) and 1(*d*) show the wavenumber and phase speed comparisons. The extended undular bore wavenumber is 8% lower than the Korteweg–de Vries undular bore wavenumber throughout the undular bore and the phase speed of the extended undular bore is 16% smaller than the phase speed of the Korteweg–de Vries undular bore throughout the bore.

2.3. *The extended cnoidal wave solution*

While the authors could not develop modulation theory for the full extended Korteweg–de Vries equation (2.12) due to the extreme algebra involved, the steady travelling-wave solution of (2.12) can be easily found. This solution can be termed the extended cnoidal wave solution. Here we present this solution (which has constant amplitude and modulus squared m) for the scaled extended Korteweg–de Vries equation

$$\eta_t + 6\eta\eta_x + \eta_{xxx} - \alpha c_1 \eta^2 \eta_x + \alpha c_2 \eta_x \eta_{xx} + \alpha c_3 \eta\eta_{xxx} + \alpha c_4 \eta_{xxxxx} = 0. \tag{2.22}$$

The cnoidal wave solution of the Korteweg–de Vries equation (the leading-order terms in (2.22)) is (see Whitham 1974)

$$\left.\begin{aligned} \eta_0 &= d + A\,\mathrm{cn}^2(K(m)\,\theta/\pi), \\ \theta &= kx - \omega_0 t, \\ k &= \frac{\pi}{K(m)}\left(\frac{A}{2m}\right)^{\frac{1}{2}}, \\ \omega_0 &= 6kd + 2Ak(2 - m^{-1}). \end{aligned}\right\} \tag{2.23}$$

where

This represents a cnoidal wavetrain of modulus squared m and amplitude $\frac{1}{2}A$. The arbitrary constant d affects the mean height of the wavetrain. The extended solution has the form

$$\left.\begin{aligned} &\eta = \eta_0 + \alpha(\gamma_0 + \gamma_1\,\mathrm{cn}^2(K(m)\,\theta/\pi) + \gamma_2\,\mathrm{cn}^4(K(m)\,\theta/\pi)), \\ &\theta = kx - \omega t, \quad \omega = \omega_0 + \alpha\omega_1. \end{aligned}\right\} \tag{2.24}$$

where

So ω_1 represents a correction to the dispersion relation and γ_0, γ_1 and γ_2 represent corrections to the amplitude and mean height. They are given by

$$\left.\begin{aligned}
\gamma_2 &= -\tfrac{1}{4}A^2(\tfrac{1}{3}c_1+c_2+2c_3-30c_4),\\
\gamma_1 &= Ad(\tfrac{1}{3}c_1+c_3)+A^2(2-m^{-1})(\tfrac{1}{6}c_1+\tfrac{1}{6}c_2+\tfrac{2}{3}c_3-5c_4),\\
\omega_1 &= 6k\gamma_0-c_1kd^2-kA^2(1-m^{-1})(\tfrac{1}{2}c_1+\tfrac{1}{2}c_2+3c_3-27c_4)\\
&\quad +2c_3kdA(2-m^{-1})+4c_4kA^2(2-m^{-1})^2.
\end{aligned}\right\} \tag{2.25}$$

This extended cnoidal wave solution is equivalent to that of Laitone (1960) who derived an extended cnoidal wave solution for surface water waves directly from the water-wave equations (2.3). For surface water waves the constants in (2.22) are $c_1 = \frac{3}{2}$, $c_2 = \frac{23}{4}$, $c_3 = \frac{5}{2}$ and $c_4 = \frac{19}{40}$. Hence our solution (for $d = 0$ and $\gamma_0 = 0$) is

$$\left.\begin{aligned}
&\eta = A\,\mathrm{cn}^2(\theta)+\tfrac{1}{2}\alpha A^2(2-m^{-1})\,\mathrm{cn}^2(\theta)+\tfrac{3}{4}\alpha A^2\,\mathrm{cn}^4(\theta),\\
\text{where}\quad &\theta = kx-\omega t = k(x-Ut),\\
&k = \left(\frac{A}{2m}\right)^{\frac{1}{2}},\\
&U = \frac{\omega}{k} = 2A(2-m^{-1})+\alpha A^2\frac{(59m^2-59m+19)}{10m^2}.
\end{aligned}\right\} \tag{2.26}$$

Laitone's solution for the surface elevation (his (4.16)) is

$$\left.\begin{aligned}
&\frac{\eta}{h} = \frac{a}{h}\mathrm{cn}^2(\alpha X)-\frac{3}{4}\left(\frac{a}{h}\right)^2\mathrm{cn}^2(\alpha X)+\frac{3}{4}\left(\frac{a}{h}\right)^2\mathrm{cn}^4(\alpha X),\\
\text{where}\quad &\alpha X = \frac{x}{h}\left(\frac{3}{4k^2}\frac{a}{h}\right)^{\frac{1}{2}}\left(1-\left(\frac{a}{h}\right)\frac{7k^2-2}{8k^2}\right),
\end{aligned}\right\} \tag{2.27}$$

and the modulus k^2 is m in our notation. To see the equivalence of these two expressions, (2.27) must be rescaled, i.e.

$$\left.\begin{aligned}
&\frac{x}{h}\to\frac{x}{h}\left(\frac{2}{3}\right)^{\frac{1}{2}},\\
&\frac{a}{h}\to\frac{a}{h}+2\left(\frac{a}{h}\right)^2\left(\frac{7k^2-2}{8k^2}\right).
\end{aligned}\right\} \tag{2.28}$$

Hence (2.27) becomes

$$\left.\begin{aligned}
&\frac{\eta}{h} = \frac{a}{h}\mathrm{cn}^2(\alpha X)+\left(\frac{a}{h}\right)^2\left(\frac{2k^2-1}{2k^2}\right)\mathrm{cn}^2(\alpha X)+\frac{3}{4}\left(\frac{a}{h}\right)^2\mathrm{cn}^4(\alpha X),\\
\text{where}\quad &\alpha X = \frac{x}{h}\left(\frac{a}{2k^2h}\right)^{\frac{1}{2}}.
\end{aligned}\right\} \tag{2.29}$$

Now (2.29) and (2.26) can be seen to be the same except that (2.29) is explicitly scaled by h, the water depth, while (2.26) is implicitly scaled by h. The second-order expressions for wave speed cannot be explicitly compared because Laitone's solution is in a moving frame of reference, his x velocity $u(x, y)$ is the sum of the wavespeed and the fluid velocity. The constant part of $u(x, y)$ (see his (4.18)) is not quite the wavespeed as it contains terms such as the Stokes' drift. If $u(x, y)$ is calculated from (2.4) and (2.7) then Laitone's (4.18) is obtained.

3. Resonant flow over topography

Consider the two-dimensional flow of a stratified fluid over a localized topography. The flow will be described by a horizontal coordinate X, a vertical coordinate z and a time T, where these coordinates have been non-dimensionalized by a lengthscale h_1, a typical vertical dimension and a timescale N_1^{-1}, N_1 being a typical value of the Brunt–Väisälä frequency. Let us assume that the basic flow state has a constant horizontal velocity of magnitude V in the X-direction, a non-dimensional density $\rho_0(z)$ (non-dimensionalized by a typical density) and a non-dimensional pressure $p_0(z)$, where $p_{0_z} = -\rho_0$. The topography is given by

$$z = -h + \alpha\beta G(\beta^{\frac{1}{2}}X), \tag{3.1}$$

where $\alpha = a/L, \beta = (h_1/L)^2$, a being a typical amplitude of the topography and L a typical horizontal lengthscale. The topography is assumed to be localized, so that $g \to 0$ as $X \to \pm\infty$. The flow will be considered in the weakly nonlinear, long-wave limit; hence $\alpha \ll 1, \beta \ll 1$. We shall further restrict the flow to the particular case when the imposed upstream flow velocity is near a linear long-wave velocity for the fluid. In this case, linear theory predicts a singular solution as energy cannot propagate away from the topography. By including the bottom topography (3.1) into the derivation of the extended Korteweg–de Vries equation (see §2, the velocity potential (2.4) must be modified to allow for the boundary condition (3.1)), it can be shown in a similar manner to Melville & Helfrich (1987) (for two-layer flow) and Akylas (1984), Cole (1985), Lee (1985) and Grimshaw & Smyth (1986) for the forced Korteweg–de Vries equation that the equation governing this flow is the forced extended Korteweg–de Vries equation

$$\begin{aligned} -u_t - \Delta u_x + 6uu_x + u_{xxx} - \alpha c_1 u^2 u_x + \alpha c_2 u_x u_{xx} + \alpha c_3 u u_{xxx} + \alpha c_4 u_{xxxxx} \\ + \alpha c_5 G\eta_x + \alpha c_6 \eta G_x + \alpha c_7 G_{xxx} + (1 + \alpha c_8 \Delta) G_x(x) = 0. \end{aligned} \tag{3.2}$$

In the present work, the initial condition

$$u(x, 0) = 0 \tag{3.3}$$

will be used, which corresponds to switching on the forcing at $t = 0$. Equation (3.2) represents a balance between nonlinearity and dispersion, which, since the flow is resonant and produces a response of $O(\alpha^{\frac{1}{2}})$, requires $\beta = \alpha^{\frac{1}{2}}$. The functions u and $G(x)$, the detuning parameter Δ and the coordinates x and t are related to the physical vertical displacement Y, the physical bottom topography, the imposed upstream flow velocity and the physical horizontal space and time coordinates by

$$\left.\begin{aligned} t = \lambda c_n \beta^{\frac{1}{2}} \alpha^{\frac{1}{2}} T, \quad x = \beta^{\frac{1}{2}} X, \\ Y = \alpha^{\frac{1}{2}} \frac{6\lambda}{\mu} u\phi_n(z), \quad V = c_n(1 + \alpha^{\frac{1}{2}}\lambda\Delta), \\ I_n G = \frac{\mu}{12\lambda^2} \rho_0 c_n^2 \phi_{nz}(-h) G(\beta^{\frac{1}{2}} X), \end{aligned}\right\} \tag{3.4}$$

where $\phi_n(z)$ is the modal function, c_n the linear phase speed for the resonantly forced long-wave mode and $I_n, \mu, \lambda, c_1, \ldots, c_8$ are given by integrals of ϕ_n (see Gear & Grimshaw 1983; Grimshaw & Smyth 1986; Melville & Helfrich 1987), the values of which will be quoted for specific stratifications later. Equation (3.2) also describes the flow produced by a two-dimensional force, such as a moving pressure distribution on the surface of a fluid of constant density (see Akylas 1984; Cole 1985; Lee 1985; Wu 1987; Lee *et al.* 1989). In this case, the function $G(x)$ is given by an expression similar to that in (3.4) which involves this force.

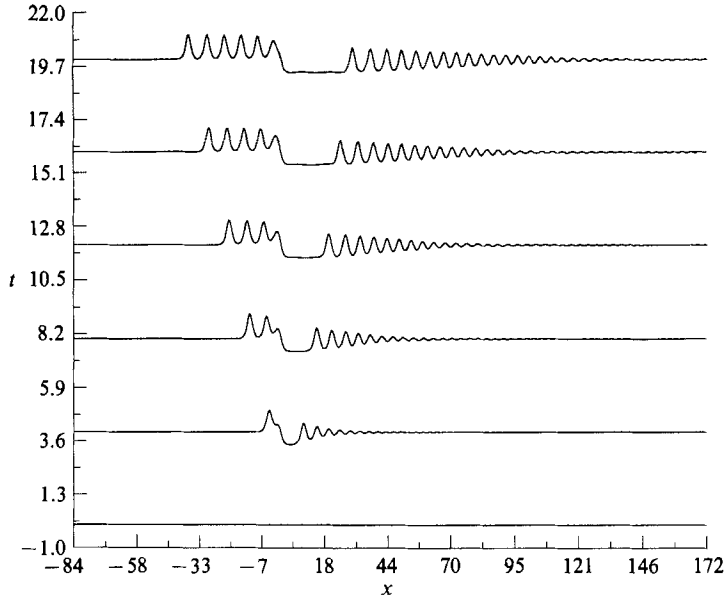

FIGURE 2. Numerical solution η of the forced extended Korteweg–de Vries equation for $\alpha c_1 = 0.2$, $\alpha c_8 = 0.05$, $\Delta = 0$, $g_0 = 1$ at time intervals of 4 up to $t = 20$.

As in Grimshaw & Smyth (1986) and Smyth (1987, 1988) it is assumed that the forcing function $G(x)$ is of the form

$$G(x) = g_0 G'(x') \quad (x' = \xi x), \tag{3.5}$$

where the function G' is taken to have the following properties: $G'(x') \geqslant 0$ for all x', G' has a maximum value of 1 at $x' = 0$ and $G' \to 0$ as $x' \to \pm\infty$. The parameter ξ measures the lengthscale of the forcing.

Numerical solutions of (3.2) are obtained using the pseudospectral method of Fornberg & Whitham (1978) (see their §2). In this method $u(x,t)$ is transformed into discrete Fourier space with respect to x (i.e. $F(u)$) and derivatives with respect to x appear as discrete Fourier transforms as well. We use the same definitions as Fornberg & Whitham (see their (7) and (8)) and obtain the following differenced version of (3.2)

$$\begin{aligned} u(x,t-\mathrm{d}t) - u(x,t+\mathrm{d}t) + 2\mathrm{i}\,\mathrm{d}t\, F^{-1}(vF(u))\,(6u - \Delta - \alpha c_1 u^2 + \alpha c_5 G) - \alpha c_2 F^{-1}(v^2 F(u))) \\ - 2\mathrm{i}F^{-1}(\sin(v^3\,\mathrm{d}t)\,F(u))\,(1+\alpha c_3 u) + 2\alpha c_4 F^{-1}(\sin(v^5\,\mathrm{d}t)\,F(u)) \\ + 2\,\mathrm{d}t\, G_x(1+\alpha c_8 \Delta) + 2\,\mathrm{d}t\,\alpha c_7 G_{xxx} = 0, \end{aligned} \tag{3.6}$$

where the discrete inverse transform is a summation over the wavenumbers v (compare this with (10) in Fornberg & Whitham). The forcing function used is

$$G = g_0 \operatorname{sech}^2 \xi x. \tag{3.7}$$

It was shown by Grimshaw & Smyth (1986) and Smyth (1987) that for broad forcings (ξ small), the solution of (3.2) depends only on the value of g_0 and not on the particular shape of the forcing function G.

Using the method of Smyth (1987), the solution of (3.2) for the particular case when only higher-order nonlinearity is present (i.e. $c_2 = c_3 = c_4 = c_5 = c_6 = c_7 = 0$) will now be found. This equation is

$$-u_t - \Delta u_x + 6uu_x + u_{xxx} - \alpha c_1 u^2 u_x + (1+\alpha c_8 \Delta)\, G_x = 0. \tag{3.8}$$

A numerical solution of this equation for $\Delta = 0$, $g_0 = 1$, $\alpha c_1 = 0.2$ and $\alpha c_8 = 0.05$ (this ratio of c_1 and c_8 represents surface water waves) at time intervals of 4 is shown in figure 2. When the forcing is switched on, the surface elevation is zero. As time goes on, three distinct solution regions develop; a modulated, unsteady wavetrain upstream of the forcing, an essentially flat depression downstream of the forcing and a modulated wavetrain following this depression, which brings the solution back to zero. Smyth (1987) used the modulation equations for the Korteweg–de Vries equation to find the solution of the forced Korteweg–de Vries equation. These modulation equations can be used as the forcing is localized and hence G is non-zero only in some finite region. It was shown that the upstream wavetrain for the forced Korteweg–de Vries equation consisted of a partial undular bore with modulus squared m in the range $0 \leqslant m_0 \leqslant m \leqslant 1$ and which had zero mean height at its leading edge. The lower modulus m_0 was chosen so that all the characteristics of the simple wave propagated upstream (away from the forcing). The downstream wavetrain was shown to be a full undular bore with zero mean height at its leading edge. These solutions will be extended to (3.8) by using the full undular bore solution (2.21) on setting x to $-x$ to take account of the change of sign of u_t in (3.8).

Setting $B = 0$ in (2.21), the wavetrain upstream of the forcing is given by

$$\left.\begin{aligned} a &= Am - \tfrac{1}{6}\alpha c_1 A^2 m(1-m), \\ \beta &= Am - A + 2A\frac{E(m)}{K(m)} + \tfrac{1}{18}\alpha c_1 A^2\left[2 - 5m + 3m^2 + 2(2m-1)\frac{E(m)}{K(m)}\right], \\ k &= \frac{\pi A^{\frac{1}{2}}}{K(m)}\left[1 - \frac{\alpha c_1}{12}A\right], \\ \text{where}\quad \frac{x}{t} &= \Delta - A(1+m)(2-\tfrac{1}{3}\alpha c_1 A) + \frac{2Am(1-m)K(m)}{E(m)-(1-m)K(m)}(2-\tfrac{1}{3}\alpha c_1 A), \\ m_0 &\leqslant m \leqslant 1. \end{aligned}\right\} \tag{3.9}$$

For this wavetrain to propagate only upstream, the minimum modulus squared m_0 is chosen so that all the characteristics Q of the expansion fan propagate upstream. Hence m_0 is the solution of

$$0 = \Delta - A(1+m_0)(2-\tfrac{1}{3}\alpha c_1 A) + \frac{2Am_0(1-m_0)K(m_0)}{E(m_0)-(1-m_0)K(m_0)}(2-\tfrac{1}{3}\alpha c_1 A). \tag{3.10}$$

Similarly, setting $A = 0$ in (2.21), the wavetrain downstream of the forcing is given by

$$\left.\begin{aligned} a &= |B|\, m - \tfrac{1}{6}\alpha c_1 B^2 m(1-m), \\ \beta &= 2B - Bm - 2B\frac{E(m)}{K(m)} + \tfrac{1}{18}\alpha c_1 B^2\left[2 - 5m + 3m^2 + 2(2m-1)\frac{E(m)}{K(m)}\right], \\ k &= \frac{\pi(|B|)^{\frac{1}{2}}}{K(m)}[1 - \tfrac{1}{12}\alpha c_1 B], \\ \text{where}\quad \frac{x}{t} &= \Delta - 4B + 2Bm + \tfrac{1}{3}\alpha c_1 B^2[2-m] - \frac{2Bm(1-m)K(m)}{E(m)-(1-m)K(m)}[2 - \tfrac{1}{3}\alpha c_1 B] \\ 0 &\leqslant m \leqslant 1, \quad \Delta - 2B + \tfrac{1}{3}\alpha c_1 B^2 \leqslant \frac{x}{t} \leqslant \Delta - 12B + 2\alpha c_1 B^2. \end{aligned}\right\} \tag{3.11}$$

For this wavetrain to propagate downstream, we require $B < 0$.

The solutions (3.9) and (3.11) for the upstream and downstream wavetrains are not complete as the values of A and B have not yet been determined. It is the parameters A and B which link the upstream and downstream wavetrains to the forcing. The solutions (3.9) and (3.11) were determined from the modulation equations for the extended Korteweg–de Vries equation and hence do not contain any direct information about the forcing. Smyth (1987) obtained approximations to A and B which yielded solutions in good agreement with numerical solutions of the forced Korteweg–de Vries equation. These approximations will be extended here to the forced extended Korteweg–de Vries equation. Full details of this method can be found in Smyth (1987).

The simple wave solutions (3.9) and (3.11) have reduced the forcing to a discontinuity at $x = 0$. To link the upstream and downstream solutions, a jump condition across the forcing needs to be found. This jump condition will link the mean levels just upstream and just downstream of the forcing and is determined by the steady solution of (3.8) which approaches constants as $x \to \pm\infty$. To match with the upstream and downstream solutions, the constant as $x \to -\infty$ must be positive and the constant as $x \to \infty$ must be negative. The steady solution is the solution of

$$-\Delta u_x + 6uu_x - \alpha c_1 u^2 u_x + u_{xxx} + (1 + \alpha c_8 \Delta) G_x(x) = 0. \tag{3.12}$$

In general, this equation is difficult to solve, but it can easily be solved in two limits; a broad forcing for which ξ is small and a δ-function forcing, for which ξ is large.

For a broad forcing, the dispersive term u_{xxx} in (3.12) can be neglected. It can then be found that the steady solution which approaches the appropriately signed constants as $x \to \pm\infty$ and is continuous at $x = 0$ is

$$u_S = \begin{cases} \frac{1}{6}[\Delta + (1 + \frac{1}{2}\alpha c_8 \Delta)(12(g_0 - G))^{\frac{1}{2}}] + \frac{1}{216}\alpha c_1 [\Delta^2 + \Delta(12(g_0 - G))^{\frac{1}{2}} + 4(g_0 - G)] & (x \leqslant 0), \\ \frac{1}{6}[\Delta - (1 + \frac{1}{2}\alpha c_8 \Delta)(12(g_0 - G))^{\frac{1}{2}}] + \frac{1}{216}\alpha c_1 [\Delta^2 - \Delta(12(g_0 - G))^{\frac{1}{2}} + 4(g_0 - G)] & (x \geqslant 0). \end{cases} \tag{3.13}$$

Hence $u_S \to \frac{1}{6}[\Delta + (1 + \frac{1}{2}\alpha c_8 \Delta)(12g_0)^{\frac{1}{2}}] + \frac{1}{216}\alpha c_1 [\Delta^2 + \Delta(12g_0)^{\frac{1}{2}} + 4g_0]$ as $x \to -\infty$, (3.14)

and $u_S \to \frac{1}{6}[\Delta - (1 + \frac{1}{2}\alpha c_8 \Delta)(12g_0)^{\frac{1}{2}}] + \frac{1}{216}\alpha c_1 [\Delta^2 - \Delta(12g_0)^{\frac{1}{2}} + 4g_0]$ as $x \to +\infty$. (3.15)

For u_S to approach a positive constant as $x \to -\infty$ and a negative constant as $x \to \infty$, we require

$$-(12g_0)^{\frac{1}{2}} + 6\alpha c_8 g_0 - \tfrac{1}{9}\alpha c_1 g_0 \leqslant \Delta \leqslant (12g_0)^{\frac{1}{2}} + 6\alpha c_8 g_0 - \tfrac{1}{9}\alpha c_1 g_0. \tag{3.16}$$

This range of Δ is the band for which resonant flow, characterized by a large, unsteady upstream wavetrain, occurs. Outside of this range, the flow is non-resonant and is qualitatively similar to the classical linear solution (see Grimshaw & Smyth 1986). As we are concerned with the resonant solution in the present work, the non-resonant solution will not be considered further.

The limiting value (3.14) provides the initial mean height for the upstream solution (3.9). The parameter A and the modulus squared m_0 at the forcing are then the solution of

$$\begin{aligned} &\tfrac{1}{6}[\Delta + (1 + \tfrac{1}{2}\alpha c_8 \Delta)(12g_0)^{\frac{1}{2}}] + \tfrac{1}{216}\alpha c_1 [\Delta^2 + \Delta(12g_0)^{\frac{1}{2}} + 4g_0] \\ &\quad = 2A\frac{E(m_0)}{K(m_0)} - A + Am_0 + \tfrac{1}{18}(\alpha c_1 A^2)\left[3m_0^2 - 5m_0 + 2(2m_0 - 1)\frac{E(m_0)}{K(m_0)}\right], \end{aligned} \tag{3.17}$$

together with (3.10). Using the fact that α is small, we find from this that

$$A = A_0 + \alpha A_1, \tag{3.18}$$

where $$A_0 = \frac{\Delta + (12g_0)^{\frac{1}{2}}}{6(m_0 - 1 + 2(E(m_0)/K(m_0)))},$$

$$A_1 = \frac{c_1(\Delta^2 + \Delta(12g_0)^{\frac{1}{2}} + 4g_0) + 18c_8\Delta(12g_0)^{\frac{1}{2}}}{216(m_0 - 1 + 2(E(m_0)/K(m_0)))} - \frac{c_1(\Delta + (12g_0)^{\frac{1}{2}})^2[3m_0^2 - 5m_0 + 2 + 2(2m_0 - 1)(E(m_0)/K(m_0))]}{648(m_0 - 1 + (2E(m_0)/K(m_0)))^3}. \tag{3.19}$$

The minimum modulus squared m_0 is determined by (3.10) on using the expression (3.18) for Δ and the solution for the upstream wavetrain is now complete.

As well as fully resonant flow in which waves are continually generated at the forcing, the solution (3.9), (3.10) and (3.18) also gives the transition to subcritical flow. When

$$\Delta = -\tfrac{1}{2}(12g_0)^{\frac{1}{2}} + \tfrac{3}{2}\alpha c_8 g_0 + \tfrac{1}{36}\alpha c_1 g_0, \tag{3.20}$$

$m_0 = 0$ and the upstream wavetrain is a full undular bore. For Δ in the range

$$-(12g_0)^{\frac{1}{2}} + 6\alpha c_8 g_0 - \tfrac{1}{9}\alpha c_1 g_0 \leqslant \Delta < -\tfrac{1}{2}(12g_0)^{\frac{1}{2}} + \tfrac{3}{2}\alpha c_8 g_0 + \tfrac{1}{36}\alpha c_1 g_0, \tag{3.21}$$

$m_0 = 0$ and the upstream solution is a full undular bore which propagates upstream. So in this range of Δ, no waves are generated at the forcing. After the bore has passed, there is a non-zero mean level in u (which is positive). The upstream solution for Δ in the range (3.21) is a transition solution from fully resonant flow, in which waves are continually generated at the forcing, to non-resonant subcritical flow in which there is no upstream disturbance.

Similarly, matching the mean level of the downstream solution (3.11) at its trailing edge, where $m = 1$, to the limiting value (3.15) gives

$$B = \tfrac{1}{6}[\Delta - (1 + \tfrac{1}{2}\alpha c_8 \Delta)(12g_0)^{\frac{1}{2}}] + \tfrac{1}{216}\alpha c_1[\Delta^2 + 4g_0 - \Delta(12g_0)^{\frac{1}{2}}], \tag{3.22}$$

which completes the downstream solution. Between the trailing edge of the downstream wavetrain and the forcing, the solution is (3.13) for $x \geqslant 0$.

If for Δ in the range

$$-(12g_0)^{\frac{1}{2}} + 6\alpha c_8 g_0 - \tfrac{1}{9}\alpha c_1 g_0 \leqslant \Delta < -\tfrac{1}{2}(12g_0)^{\frac{1}{2}} + \tfrac{3}{2}\alpha c_8 g_0 - \tfrac{7}{36}\alpha c_1 g_0, \tag{3.23}$$

m is allowed to take all values $0 \leqslant m \leqslant 1$, then part of the expansion fan will propagate upstream. For $\Delta = -\tfrac{1}{2}(12g_0)^{\frac{1}{2}} + \tfrac{3}{2}\alpha c_8 g_0 - \tfrac{7}{36}\alpha c_1 g_0$, the solution at the trailing edge of the expansion fan has zero velocity. For Δ in the range (3.23), the expansion fan (3.11) could be stopped at a value of m for which the trailing characteristic has zero velocity, as was done for the upstream solution. However, as Δ decreases, the solution must merge with the non-resonant solution, which has a stationary lee wavetrain downstream of the forcing. A restricted expansion fan will not do this as the phase velocity at the forcing does not approach zero as the lower limit in (3.23) is approached. Also the numerical results of Grimshaw & Smyth (1986) for the forced Korteweg–de Vries equation show that for $\Delta < -\tfrac{1}{2}(12g_0)^{\frac{1}{2}}$, a stationary lee wavetrain preceded by a transient front develops downstream of the forcing. The downstream solution for Δ in the range (3.23) will then consist of a stationary wavetrain of modulus m_l proceeded by an expansion fan of the form (3.11) in which the modulus varies in the range $m_l \geqslant m \geqslant 0$.

Matching between the stationary lee wavetrain and the expansion fan (3.11) gives β_l and a_l for the lee wavetrain as

$$\beta_l = 2B - Bm_l - 2B\frac{E(m_l)}{K(m_l)} + \tfrac{1}{18}\alpha c_1 B^2\left[3m_l^2 - 5m_l + 2 + 2(2m_l - 1)\frac{E(m_l)}{K(m_l)}\right]$$

$$= \tfrac{1}{6}[\Delta - (1 + \tfrac{1}{2}\alpha c_8\,\Delta)(12g_0)^{\frac{1}{2}}] + \tfrac{1}{216}\alpha c_1[\Delta^2 + 4g_0 - \Delta(12g_0)^{\frac{1}{2}}], \tag{3.24}$$

$$a_l = |B|\, m_l - \tfrac{1}{6}\alpha c_1 B^2 m_l(1 - m_l). \tag{3.25}$$

From the expression given in (2.17) for the phase velocity U, we find that for this velocity to be zero in the lee wavetrain, we require

$$B = \frac{\Delta}{2(2-m_l)} - \frac{\alpha c_1}{24}\frac{\Delta^2}{(2-m_l)^3}\left[m_l^2 + m_l - 2 + 2(2-m_l)\frac{E(m_l)}{K(m_l)}\right]. \tag{3.26}$$

The modulus squared m_l and the parameter B are then the solution of (3.24) and (3.26). From (3.11), the wavenumber of the lee wavetrain is

$$k_l = \frac{\pi(|B|)^{\frac{1}{2}}}{K(m_l)}[1 - \tfrac{1}{12}\alpha c_1 B]. \tag{3.27}$$

The lee wavetrain downstream of the forcing for Δ in the range (3.23) is then given by (3.24), (3.25) and (3.27). From (3.11), this lee wavetrain occurs in the range

$$0 \leqslant \frac{x}{t} \leqslant \Delta - 4B + 2Bm_l + \tfrac{1}{3}\alpha c_1 B^2[2 - m_l] - \frac{2Bm_l(1-m_l)K(m_l)}{E(m_l) - (1-m_l)K(m_l)}[2 - \tfrac{1}{3}\alpha c_1 B]. \tag{3.28}$$

Ahead of this lee wavetrain, there is an expansion fan given by (3.11), but with m in the range $0 \leqslant m \leqslant m_l$. This expansion fan is a transient front which brings the solution back to zero from the lee wavetrain. The solution in the range (3.23) is the nonlinear counterpart of the linear subcritical solution which has a stationary (linear) lee wavetrain preceded by a transient wavetrain.

In the case of the forced Korteweg–de Vries equation ($c_1 = c_8 = 0$), both the upstream and downstream wavetrains undergo transition to the non-resonant solution at the same value of Δ (see (3.21) and (3.23)). However, for the forced extended Korteweg–de Vries equation, the upstream solution starts the transition to the non-resonant solution at a higher value of Δ than the downstream solution.

We see from (3.9) that the waves at the leading edge of the upstream wavetrain are solitons ($m = 1$). The amplitude of these solitons is given by (3.9), (3.10), (3.18) and (3.19). Figure 3(*a*) shows a comparison of the upstream soliton amplitudes as predicted from modulation theory for the forced extended Korteweg–de Vries and forced Korteweg–de Vries equations over the range of the detuning parameter, Δ, for which the solution is resonant. In this example $g_0 = 1$, $\alpha c_1 = 0.2$ and $\alpha c_8 = 0.05$ (which represents surface water waves). For negative delta (where the fluid velocity is less than the linear wave speed), the soliton amplitudes are very similar. However, for positive delta (where the fluid velocity is greater than the linear wave speed) there is more variation with the soliton amplitude corresponding to the extended Korteweg–de Vries theory being greater than that of the Korteweg–de Vries theory.

Figure 3(*b*) shows a comparison of the modulus squared, m_0 (given by (3.10)), at which the upstream cnoidal wavetrain begins between the predictions of modulation theory for the forced extended Korteweg–de Vries and forced Korteweg–de Vries

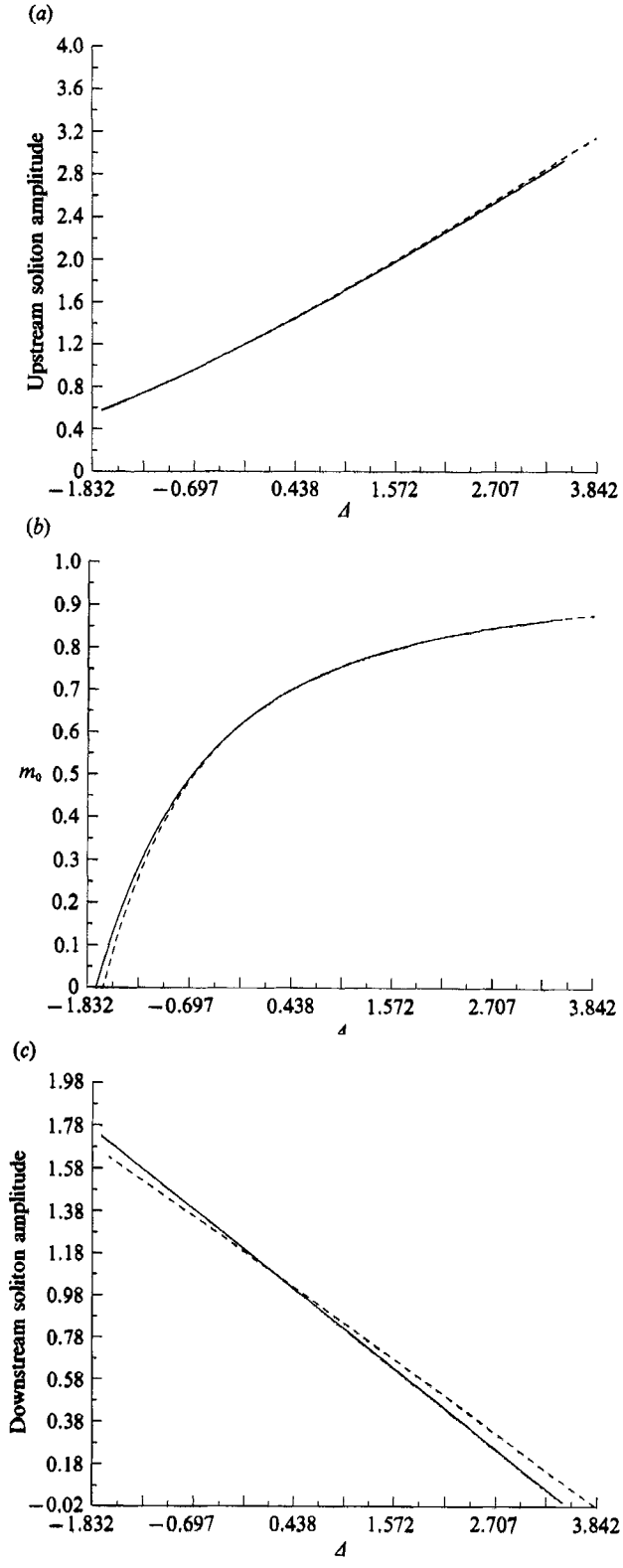

FIGURE 3. (*a*) The upstream soliton amplitude from modulation theory for resonant flow over topography versus the detuning parameter Δ. Compared are – – –, the forced extended Korteweg–de Vries equation for $\alpha c_1 = 0.2$ and $\alpha c_g = 0.05$ and ——, the forced Korteweg–de Vries equation. Also shown for the same situation as (*a*) is (*b*) the modulus squared, m_0, at which the upstream wavetrain begins and (*c*) the downstream soliton amplitude.

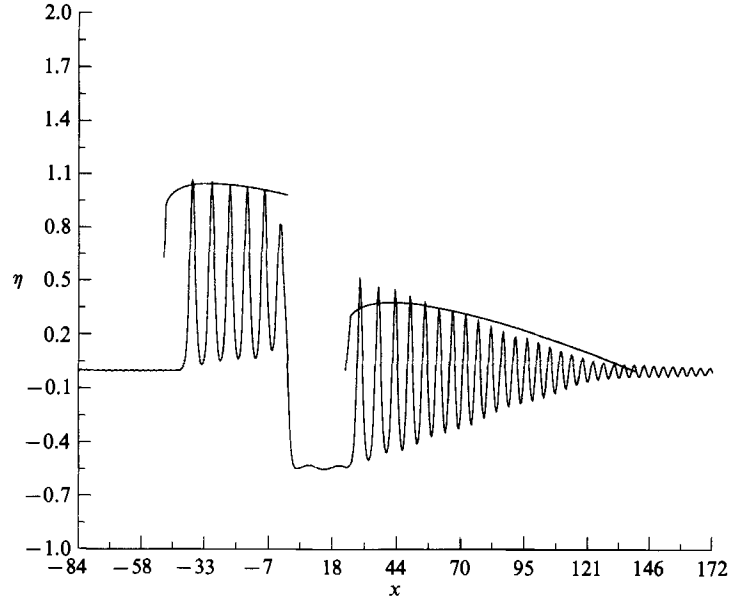

FIGURE 4. The numerical solution η of the forced extended Korteweg–de Vries equation for resonant flow over topography for $\alpha c_1 = 0.2$, $\alpha c_3 = 0.05$, $g_0 = 1$, $\Delta = 0$ and $t = 20$. Also shown is the wave envelope for the upstream and downstream cnoidal wavetrains from extended modulation theory.

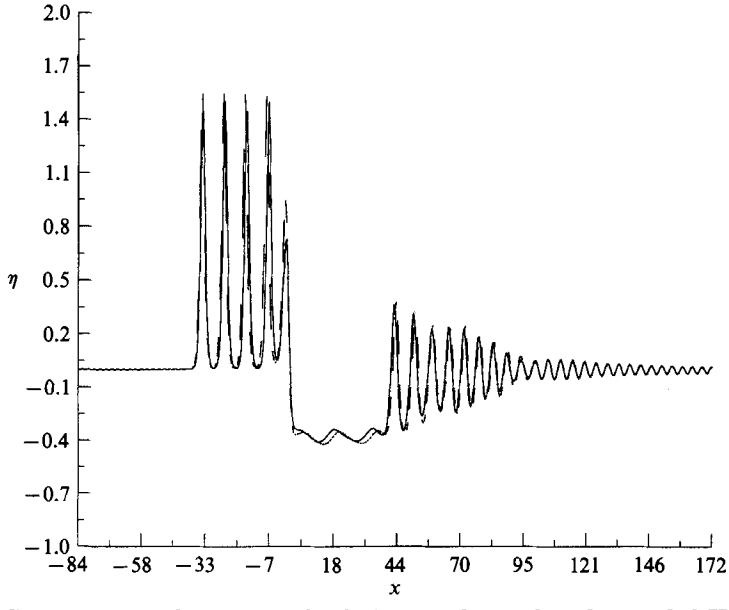

FIGURE 5. Comparison of the numerical solutions η of ---, forced extended Korteweg–de Vries equation and ——, the forced Korteweg–de Vries equation for resonant flow over topography. The parameters are $g_0 = 1$, $\alpha c_1 = 0.2$, $\alpha c_3 = 0.05$, $\Delta = 1.0$ and $t = 20$.

equations. The parameters are the same as for figure 3(*a*). For negative delta the modulus squared m_0 as given by the extended Korteweg–de Vries theory is less than that of Korteweg–de Vries theory. For positive delta the modulus squared m_0 of the extended Korteweg–de Vries theory is similar to that of Korteweg–de Vries theory.

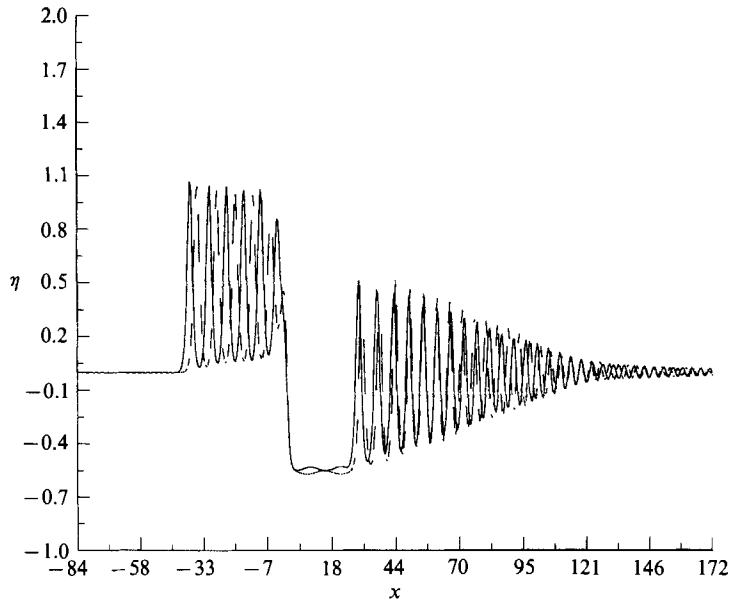

FIGURE 6. Comparison of the numerical solutions η of – – –, the forced full extended Korteweg–de Vries equation and ——, the forced Korteweg–de Vries equation for resonant flow over topography. The parameters are $g_0 = 1$, $\alpha c_1 = 0.15$, $\Delta = 0$ and $t = 20$.

At delta equal to zero (when the fluid velocity is equal to the linear phase velocity), the modulus squared m_0 as predicted by both theories is the same.

The downstream undular bore solution (3.11) has solitons ($m = 1$) at its trailing edge. Figure 3(*c*) shows a comparison of the downstream soliton amplitudes for the same situation as figures 3(*a*) and 3(*b*). For negative delta the downstream soliton amplitude as predicted by extended Korteweg–de Vries theory is smaller than the Korteweg–de Vries theory while for positive delta the downstream soliton amplitude as predicted by extended Korteweg–de Vries theory is greater than Korteweg–de Vries theory.

We shall now present some results of the numerical solution of (2.13), the extended Korteweg–de Vries equation with only the higher-order nonlinearity present and of (2.12), the full extended Korteweg–de Vries equation for surface water waves (the higher-order coefficients are given by (2.8)). The numerical solutions are calculated using the pseudospectral method of Fornberg & Whitham (1978) (see (3.6)). The forcing used is a broad obstacle with $G(x) = g_0 \operatorname{sech}^2(x)$.

Figure 4 shows the numerical solution of the forced extended Korteweg–de Vries equation for $\Delta = 0$, $g_0 = 1$, $\alpha c_1 = 0.2$, $\alpha c_8 = 0.05$ and time = 20. Also drawn are the wave envelopes of the upstream and downstream cnoidal wavetrains as predicted by modulation theory for the forced extended Korteweg–de Vries equation. These wave envelopes are $\beta + a$ with β given by (3.9) and (3.11) for the upstream and downstream wavetrains respectively. The agreement between theory and numerical results is excellent with some slight disagreement in the region of the obstacle.

The difference between the numerical solutions of the forced extended Korteweg–de Vries equation and the forced Korteweg–de Vries equation is slight (and barely discernible graphically) for Δ near zero, but increases as Δ increases. Figure 5 shows a comparison between the numerical solutions of the forced extended

Korteweg–de Vries equation and the forced Korteweg–de Vries equation for $g_0 = 1$, $\alpha c_1 = 0.2$, $\alpha c_8 = 0.05$, $t = 20$ and $\Delta = 1.0$. The solution of the extended equation shows some discernible changes. First, the amplitude of the leading edge of the upstream wavetrain (the lead soliton) is slightly higher than the Korteweg–de Vries amplitude. Also the waves are travelling slightly faster upstream. This difference in wavetrain properties is in agreement with the predictions of modulation theory. Figure 3(*a*) shows that the upstream soliton amplitude is increased while (3.9) gives the velocity of each cnoidal wave in the upstream undular bore. In particular, the lead soliton's velocity is

$$U = \Delta - 4A_0 + \tfrac{2}{3}\alpha c_1 A_0^2 - 4\alpha A_1, \tag{3.29}$$

where A_0, A_1 are defined in (3.19). Because A_1 is positive (figure 3(*a*) shows that the upstream soliton amplitude is increased for positive Δ) and larger than the other higher-order term, this represents a faster velocity (upstream) than for a Korteweg–de Vries soliton. Downstream the wave amplitude is increased (see figure 3(*c*) for positive Δ) and the waves are travelling faster.

Figure 6 shows a comparison between the numerical solutions for the forced full extended Korteweg–de Vries equation for surface water waves and the forced Korteweg–de Vries equation for $g_0 = 1$, $\alpha c_1 = 0.15$, $t = 20$ and $\Delta = 0$. For surface water waves $c_1 = 1$, $c_2 = \frac{23}{6}$, $c_3 = \frac{5}{3}$, $c_4 = \frac{19}{40}$, $c_5 = -\frac{4}{3}$, $c_6 = -\frac{7}{6}$, $c_7 = 0$ and $c_8 = \frac{1}{4}$. Upstream, the solution of the full extended Korteweg–de Vries equation shows two main differences with the Korteweg–de Vries solution. First, there is an amplitude reduction and, in addition, the upstream undular bore is travelling slower. Downstream, the waves are travelling more slowly also, while little change in the downstream undular bore amplitude has occurred. The higher-order nonlinear–dispersive and higher-order dispersive terms in (2.12) then have more effect on the resonant flow solution than the higher-order nonlinear term, although the effect of none of the higher-order terms is very great until the wave amplitudes become fairly large.

4. Comparison with experiment

In this section we compare the results from modulation theory for the extended Korteweg–de Vries equation and some numerical results for the forced extended Korteweg–de Vries equation with boundary-layer viscosity included (see Smyth 1988) with some numerical and experimental results obtained by Melville & Helfrich (1987). They considered two-layer resonant flow over topography and derived a forced extended Korteweg–de Vries equation for this two-layer fluid which included the higher-order cubic nonlinearity, but not the higher-order dispersion. Experimental and numerical results were obtained for a range of parameters. Here we rescale their forced extended Korteweg–de Vries equation (2.12) derived for a two-layer fluid to our (3.8), with $c_8 = 0$, and compare their results with our modulation theory for the forced extended Korteweg–de Vries equation and the forced Korteweg–de Vries equation. Smyth (1988) considered the effect of boundary-layer viscosity on resonant flow (see his (2.12)). Extending his (2.12) to include the cubic nonlinearity also, we have that the forced extended Korteweg–de Vries equation including boundary-layer viscosity is

$$-u_t - \Delta u_x + 6uu_x + u_{xxx} - \alpha c_1 u^2 u_x + G_x - \delta V(u) = 0, \tag{4.1}$$

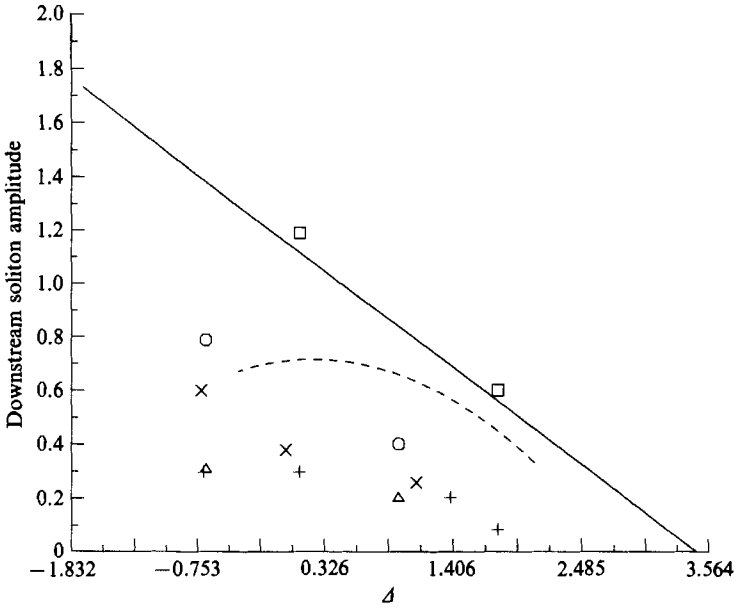

FIGURE 7. The downstream soliton amplitude for resonant flow over topography versus Δ. Modulation theory for ——, the forced Korteweg–de Vries equation and – – –, the extended forced Korteweg–de Vries equation for $\alpha c_1 = 12$. Melville & Helfrich's numerical results (□, their figure 10 and ○, their figure 5) and their experimental results (+, from figure 10 and △, from figure 5). Also shown are ×, numerical solutions of the forced extended Korteweg–de Vries equation for $\alpha c_1 = 12$ with boundary-layer viscosity $\delta = 0.06$.

where
$$\left.\begin{aligned} V(u) &= \frac{1}{2\pi}\int_{-\infty}^{\infty} (-\mathrm{i}k)^{\frac{1}{2}} \mathrm{e}^{\mathrm{i}kx} F(u)\,\mathrm{d}k, \\ F(u) &= \int_{-\infty}^{\infty} \mathrm{e}^{-\mathrm{i}k\theta} u(\theta, t)\,\mathrm{d}\theta. \end{aligned}\right\} \tag{4.2}$$

For a two-layer fluid of lower-layer density ρ_2, upper-layer density ρ_1, lower-layer depth d and total depth h, the parameter δ is given by

$$\delta = \left(\frac{\nu}{\beta^5}\right)^{\frac{1}{2}} \frac{6\sqrt{2}(\rho_1 d + \rho_2(h-d))^{\frac{1}{2}}}{d^2[h(h-d)(\rho_1+\rho_2)]^{\frac{1}{2}}[\rho_2 d + \rho_1(h-d)]}, \tag{4.3}$$

ν being the (non-dimensionalized) kinematic viscosity (see Leone, Segur & Hammack 1982; Grimshaw 1983). The densities are non-dimensionalized by the mean density of the two fluids and the depths are non-dimensionalized by the product of the depths of the two layers divided by the total depth. Solutions of the equation are compared with those of Melville & Helfrich (1987). For the results presented by Melville & Helfrich, our small parameter αc_1 ranges between approximately 4 and 14.

Hence comparison between the numerical and theoretical results is of limited value, as the extended Korteweg–de Vries equation is derived under the assumption that $\alpha c_1 \ll 1$. There are some interesting features of the solution however and these are shown in figure 7.

Figure 7 shows the downstream soliton amplitude over the range of Δ for which the flow is resonant. Shown are the modulation theory results for the forced Korteweg–de Vries equation and the forced extended Korteweg–de Vries equation for $\alpha c_1 = 12$,

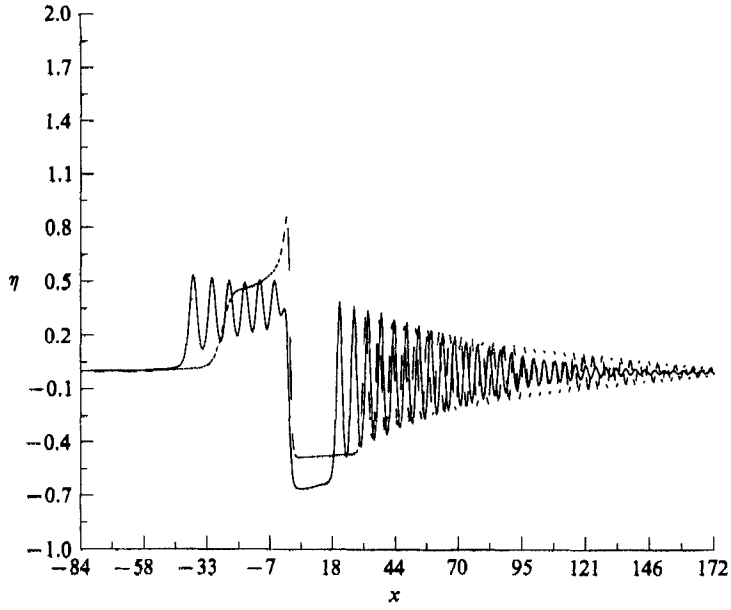

FIGURE 8. Comparison of the numerical solutions η of ---, the forced extended Korteweg–de Vries equation and ——, the forced Korteweg–de Vries equation for resonant flow over topography. Also included is boundary-layer viscosity. The parameters are $g_0 = 1$, $\alpha c_1 = 12$, $\Delta = -0.72$, $\delta = 0.06$ and $t = 20$.

Melville & Helfrich's numerical results for the Korteweg–de Vries equation (their figure 10), and their numerical solutions for the extended Korteweg–de Vries equation with $\alpha c_1 \approx 13$, and their experimental results (their figure 10 with $\alpha c_1 \approx 12$, and figure 5 with $\alpha c_1 \approx 13$). Also shown are numerical solutions for (4.1), the forced extended Korteweg–de Vries equation with boundary-layer viscosity ($\alpha c_1 \approx 12$ and $\delta \approx 0.06$, where δ was calculated from Melville & Helfrich's experimental data).

First, this figure shows very good agreement between the modulation theory solution for the forced Korteweg–de Vries equation and Melville & Helfrich's numerical forced Korteweg–de Vries results. Comparison of the results for the forced extended Korteweg–de Vries equation is only fair, but this is to be expected since the theory is being applied for values of αc_1 well outside its validity. All of the experimental results show amplitudes much smaller than any of Melville & Helfrich's numerical solutions or the results from modulation theory. However once boundary-layer viscosity is included in the forced extended Korteweg–de Vries equation, much better agreement is obtained with experiment. For $\Delta \geqslant 0$ very good agreement is obtained, while for $\Delta = -0.75$ the agreement is not as good, with the numerical result much greater than the experimental value. There are a number of possible reasons for this: (*a*) the neglected higher-order dispersive terms may be more important for Δ negative; (*b*) the theory is less valid as the amplitude increases; or (*c*) the solitons may be breaking (solitons break at amplitudes of about 0.7 which is the order of the soliton amplitude at $\Delta = -0.75$).

Figure 8 shows a comparison of the numerical solutions of the forced extended Korteweg–de Vries equation ($\alpha c_1 = 12$) and the forced Korteweg–de Vries equation. Both equations include boundary-layer viscosity, $\delta = 0.06$. There are significant qualitative differences in the solutions. Upstream, the Korteweg–de Vries solution is a modulated cnoidal wavetrain, while the extended Korteweg–de Vries solution is a

	Forced Korteweg–de Vries equation	Forced extended Korteweg–de Vries equation ($\alpha c_1 = 6$)
Modulation theory	$-1.73 < \Delta < 3.46$	$-1.56 < \Delta < 2.8$
Numerical solutions	$-2.26 < \Delta < 4.53$	$-1.69 < \Delta < 3.37$

TABLE 1. Comparison of resonant bands with numerical solutions of Melville & Helfrich (1987) (their figures 3 and 8)

non-dissipative bore described by a 'tanh' profile (see Melville & Helfrich (2.18*a*) for more details). Downstream, the extended Korteweg–de Vries solution has a shallower and longer flat depression immediately behind the obstable, while the downstream modulated cnoidal wavetrains are of similar amplitude.

In conclusion, the combination of the cubic nonlinearity and boundary-layer viscosity results in good agreement with experiment. However, care must be exercised in making definite conclusions as αc_1 is outside the range of validity of the extended Korteweg–de Vries equation, and (see the non-dissipative bore in figure 8) the effect of friction can cause solutions not described by modulation theory to develop.

Another point of interest is the size of the resonant bands. In table 1, we compare the resonant band of the modulation theory for the forced Korteweg–de Vries equation and for the forced extended Korteweg–de Vries equation (for a broad obstacle) for $\alpha c_1 = 6$. Also given are the resonant bands from Melville & Helfrich's numerical solutions of the forced Korteweg–de Vries equation and the forced extended Korteweg–de Vries equation. Comparison between modulation theory for the forced Korteweg–de Vries equation and Melville & Helfrich's numerical results shows a 23% difference in both the upper and lower band limits. Modulation theory for the forced extended Korteweg–de Vries equation gives better agreement with the numerical results. The lower band limit shows a 7% difference between modulation theory and the numerical results while the upper band limit shows a 16% variation. Again, good agreement between the theoretical and numerical results was not expected as αc_1 is not $\ll 1$.

T. R. M. would like to acknowledge support from the Australian Research Council under Grant A 48716128.

REFERENCES

AKYLAS, T. R. 1984 On the excitation of long nonlinear water waves by a moving pressure distribution. *J. Fluid Mech.* **141**, 455–466.

BAINES, P. G. 1984 A unified description of two-layer flow over topography. *J. Fluid Mech.* **146**, 127–167.

BYATT-SMITH, J. G. B. 1987 Perturbation theory for approximately integrable partial differential equations, and the change of amplitude of solitary-wave solutions of the BBM equation. *J. Fluid Mech.* **182**, 467–483.

CHOW, K. W. 1989 A second order solution for the solitary wave in a rotational flow. *Phys. Fluids* A **1**(7), 1235–1239.

COLE, S. L. 1985 Transient waves produced by flow past a bump. *Wave Motion* **7**, 579–587.

FLASCHKA, H., FOREST, M. G. & MCLAUGHLIN, D. W. 1980 Multiphase averaging and the inverse spectral solution of the Korteweg–de Vries equation. *Commun. Pure Appl. Maths* **33**, 739–784.

FORNBERG, B. & WHITHAM, G. B. 1978 A numerical and theoretical study of certain nonlinear wave phenomena. *Phil. Trans. R. Soc. Lond.* A **289**, 373–404.

GEAR, J. & GRIMSHAW, R. 1983 A second order theory for solitary waves in shallow fluids. *Phys. Fluids* **26**, 14–29.

GRIMSHAW, R. H. J. 1983 Solitary waves in density stratified fluids. In *Nonlinear Deformation Waves, IUTAM Symp., Tallinn, 1982* (ed. U. Nigel & J. Engelbrecht), pp. 431–447. Springer.

GRIMSHAW, R. H. J. & SMYTH, N. F. 1986 Resonant flow of a stratified fluid over topography. *J. Fluid Mech.* **169**, 429–464.

GUREVICH, A. V. & PITAEVSKII, L. P. 1974 Nonstationary structure of a collisionless shock wave. *Sov. Phys., J. Exp. Theor. Phys.* **38**, 291–297.

HELFRICH, K. R., MELVILLE, W. K. & MILES, J. W. 1984 On interfacial solitary waves over slowly varying topography. *J. Fluid Mech.* **149**, 305–317.

HUANG, D.-B., SIBEL, G. J., WEBSTER, W. C., WEHAUSEN, J. V., WU, D.-M. & WU, T. Y. 1982 Ships moving in the transcritical range. In *Proc. Conf. on Behaviour of Ships in Restricted Waters, Varna*, vol. 2, pp. 26-1–26-10.

KAKUTANI, T. & YAMASAKI, N. 1978 Solitary waves on a two-layer fluid. *J. Phys. Soc. Japan* **45**, 674–679.

KAUP, D. J. & NEWELL, A. C. 1978 Solitons as particles, oscillators, and in slowly changing media: a singular perturbation theory. *Proc. R. Soc. Lond.* A **361**, 413–446.

LAITONE, E. V. 1960 The second approximation to cnoidal and solitary waves. *J. Fluid Mech.* **9**, 430–444.

LEE, S.-J. 1985 Generation of long water waves by moving disturbances. PhD thesis, California Institute of Technology.

LEE, S.-J., YATES, G. T. & WU, T. Y. 1989 Experiments and analysis of upstream advancing solitary waves generated by moving disturbances. *J. Fluid Mech.* **199**, 569–593.

LEONE, C., SEGUR, H. & HAMMACK, J. L. 1982 Viscous decay of long internal solitary waves. *Phys. Fluids* **25**, 942–944.

LONG, R. R. 1956 Solitary waves in one- and two-fluid systems. *Tellus* **8**, pp. 460–471.

LUKE, J. C. 1967 A variational principle for a fluid with a free surface. *J. Fluid Mech.* **27**, 395–397.

MELVILLE, W. K. & HELFRICH, K. R. 1987 Transcritical two-layer flow over topography. *J. Fluid Mech.* **178**, 31–52.

MILES, J. W. 1979 On internal solitary waves. *Tellus* **31**, 456–462.

SMYTH, N. F. 1987 Modulation theory solution for resonant flow over topography. *Proc. R. Soc. Lond.* A **409**, 79–97.

SMYTH, N. F. 1988 Dissipative effects on the resonant flow of a stratified fluid over topography. *J. Fluid Mech.* **192**, 287–312.

WHITHAM, G. B. 1965*a* A general approach to linear and nonlinear dispersive waves using a Lagrangian. *J. Fluid Mech.* **22**, 273–283.

WHITHAM, G. B. 1965*b* Non-linear dispersive waves. *Proc. R. Soc. Lond.* A **283**, 238–261.

WHITHAM, G. B. 1967 Variational methods and applications to water waves. *Proc. R. Soc. Lond.* A **299**, 6–25.

WHITHAM, G. B. 1974 *Linear and Nonlinear Waves*. Wiley-Interscience.

WU, D. M. & WU, T. Y. 1982 Three-dimensional nonlinear long waves due to moving surface pressure. In *Proc. 14th Symp. on Naval Hydrodynamics, Ann Arbor*.

WU, T. Y. 1987 Generation of upstream advancing solitons by moving disturbances. *J. Fluid Mech.* **184**, 75–99.